National Institute of Standards and Technology
U.S. Department of Commerce

Material Characterization of Phantom Standards Developed by NIST for Quantitative Optical Medical Imaging Applications

Jeeseong Hwang, Aaron M. Goldfain, Helen Zhang, and Kimberly Briggman

2023 CIE/CORM
11.06.2023

Jeeseong Hwang

Applied Physics Division, National Institute of Standards and Technology

325 Broadway, Boulder, CO 80305 USA

jch@nist.gov

Phantom standards for optical medical devices

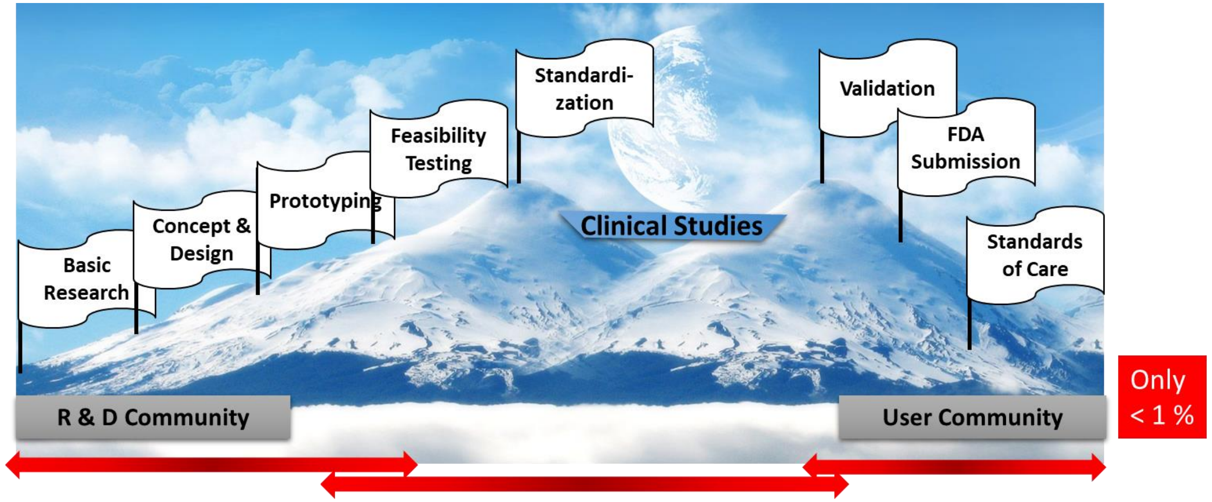

Phase 1
Discovery research
•Devices are **<u>Individually</u>** made as needed by the device lab
•Performance verification drives design decisions

Phase 2
Translational research
•Usually requires **<u>multiple device</u>** performance for QC
•GLP to GMP transition becomes challenging
•NIST traceable materials & characteristics will be essential

Phase 3
Commercial production
•Traceable, <u>rigorous validation of biological signatures and safety may be critical for</u> QC
•QC in GMP is essential in commercial production line and for user guide/training

PHANTOMS = Proficiency evaluation materials – Controlled property (e.g. homogeneous) material or artifact that is used to test and evaluate the measurement performance of different measuring systems for specific tasks.

Phantoms serve to…
- ❑ Test physical models
- ❑ Test system designs
- ❑ Verify device performance functions (SNR, CNR, etc.): "device constructed correctly?"
- ❑ Validate device capabilities for routine QC and clinical proficiency
- ❑ Inter-laboratory comparison and standardization
- ❑ Validate new techniques

This talk will focus on:

I. Diffuse optical imaging (DOI)
II. Optical coherence tomography (OCT)
III. Photoacoustic imaging (PAI)

Hwang, Ramella-Roman, and Nordstrom (Biomed Opt Exp 2012)

Type I: Standards for diffuse optical imaging (DOI)

- ❑ DOI devices, diffuse optical tomography and spatial frequency domain imager, are useful for deep tissue imaging.
- ❑ Biomarkers for *broadband* tissue diagnosis:
  - ➢ Absorption and reduced scattering coefficient spectra: $\mu_a(\lambda)$ and $\mu_s'(\lambda)$
  - ➢ Young's modulus
  - ➢ Refractive index, birefringence, etc.
- ❑ NIST has developed phantoms for the range from visible to NIR for DOI applications.
  - ➢ Base material is polydimethylsiloxane (PDMS) polymer.
  - ➢ $\mu_a(\lambda)$ and $\mu_s'(\lambda)$ are ***independently*** adjusted by carbon black particles (CBPs) and titanium dioxide particles (TDPs).
  - ➢ **Independent** control has been challenging since absorber particles scatter light too and vice versa.
  - ➢ Characterized by a NIST (wavelength-traceable) integrating sphere with the ***broadband adding double algorithm***.

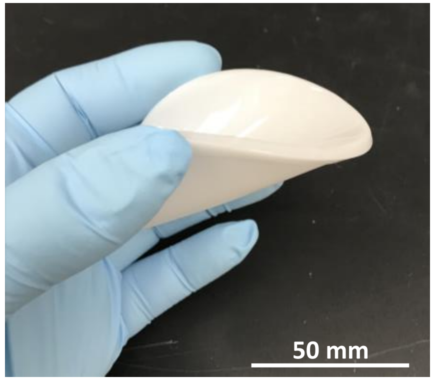

Tissue-simulating mechanical properties

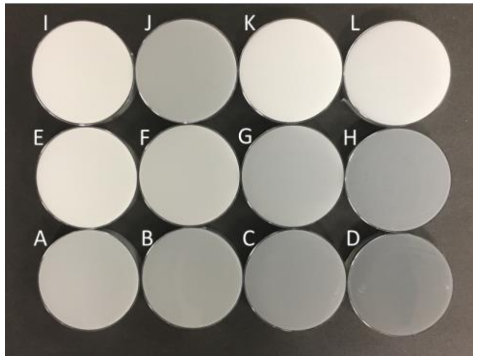

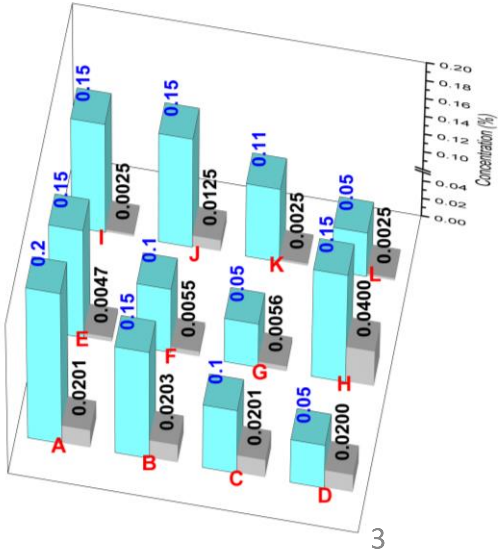

$\mu_a(\lambda)$ and $\mu_s'(\lambda)$ are **independently** adjustable

(A) $\mu_a(\lambda)$ vs concentrations

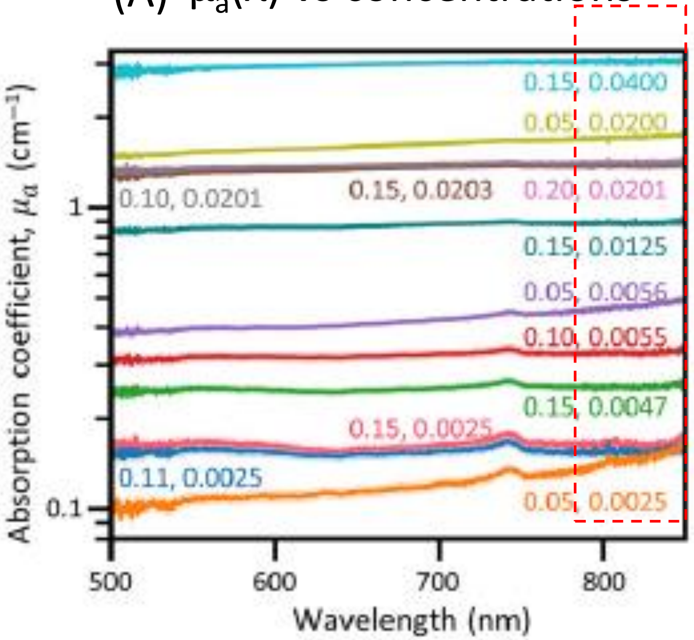

(B) $\mu_s'(\lambda)$ vs concentrations

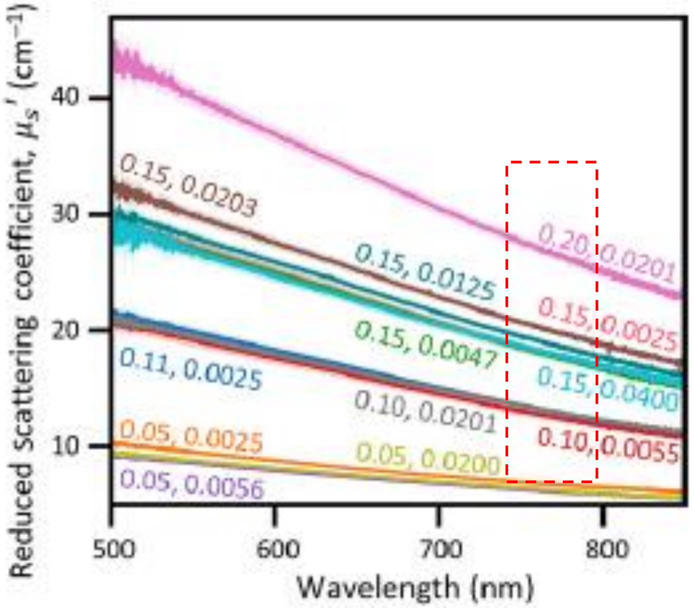

(C) NIST vs PTB

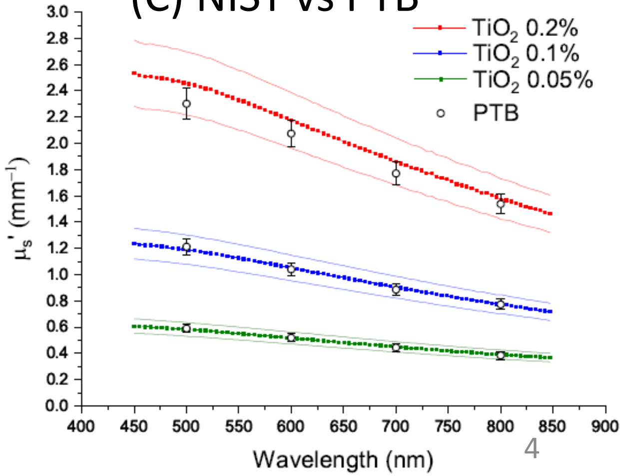

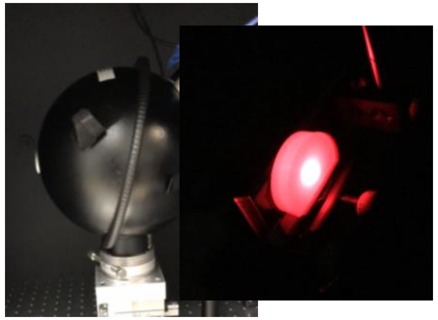

Concise tabulation of the phantom's optical properties

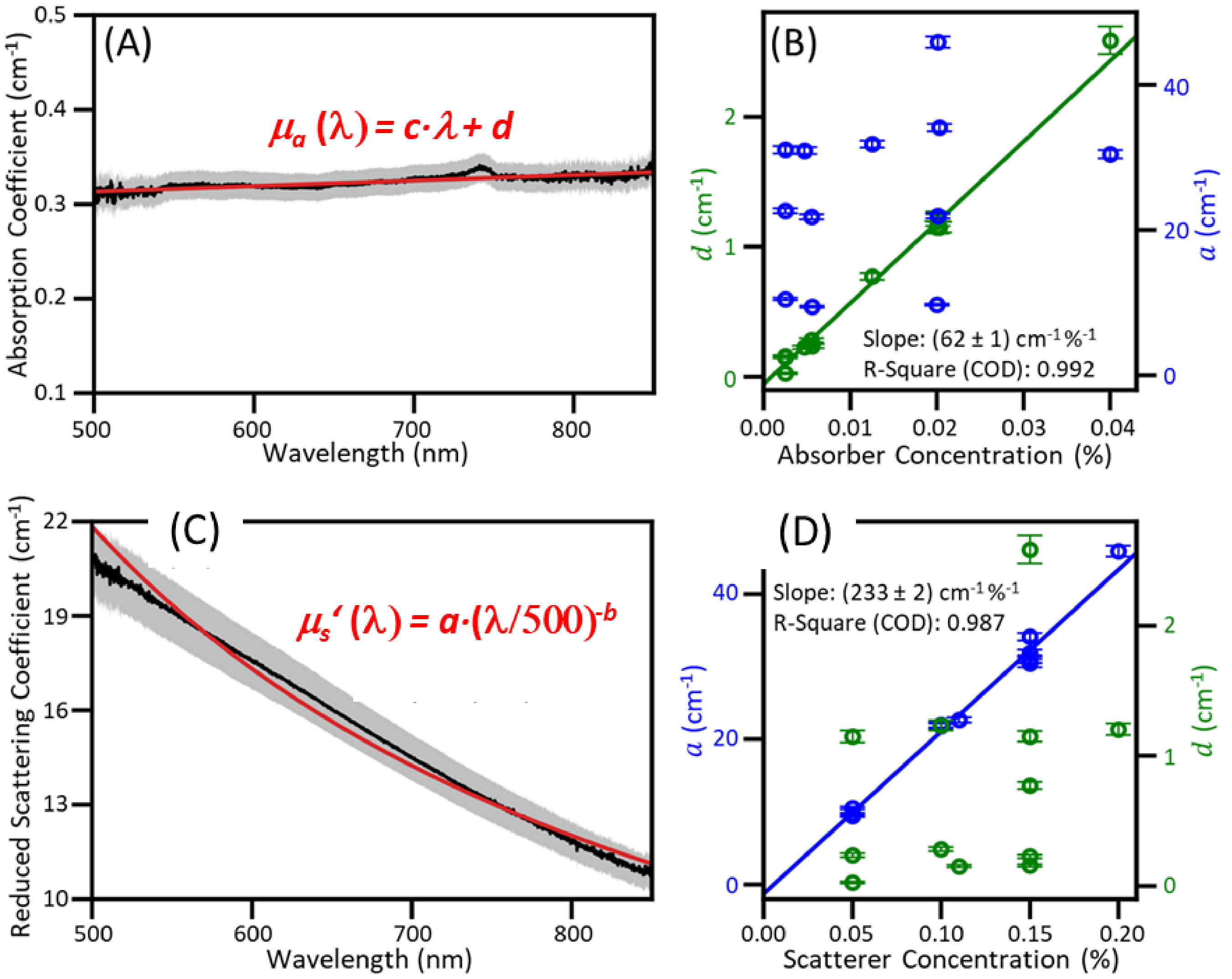

Phantoms' $\mu_s'(\lambda)$ mimics human tissues' $\mu_s'(\lambda)$

$$\mu_s'(\lambda) = a \cdot (\lambda/500)^{-b}$$

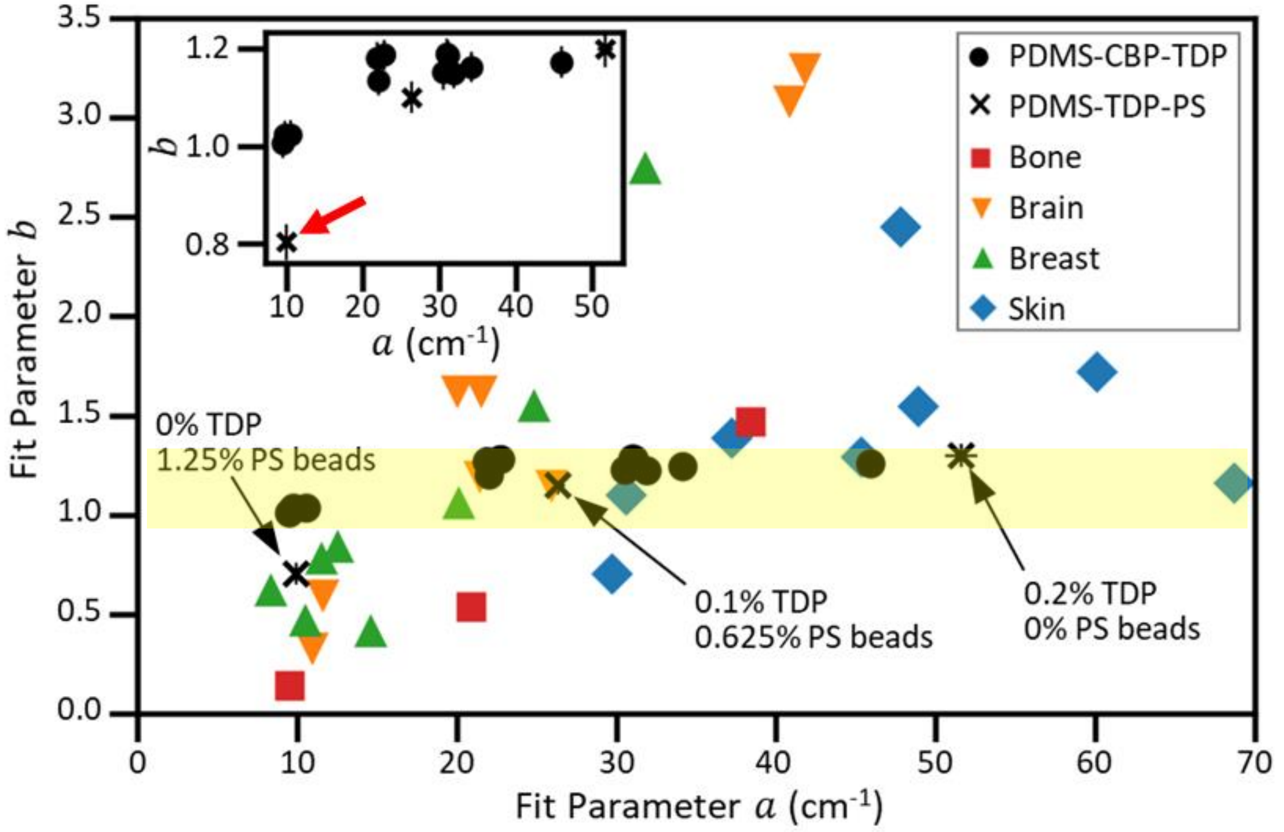

In summary, the spectral shape of $\mu_s'(\lambda)$ and $\mu_a(\lambda)$ can be tuned to mimic various types of human tissues by adjusting particle size and concentration. And tabulation with the 4 parameters provides a simple way to check the tissue-mimicking properties of the phantoms.

Raw tissue data from S. L. Jacques, "Optical properties of biological tissues: a review," Physics in Medicine and Biology **58**(14), 5007–5008 (2013).

Type II: Standards for optical coherence tomography (OCT)

- OCT provides retina diagnosis by imaging layered tissue structures.
- Sull et al reported that the intersystem comparison with different OCT devices *for the same patient* has shown variations in the results (>25% variation).
- Calibration of each OCT device is needed for results with a good measurement confidence.
- NIST has developed OCT phantom as standard reference material (SRM) for thickness and refractive index calibration of OCT.

Device	Mean foveal Thickness (µm)
Stratus OCT	214±11
Cirrus	267±14
RTVue, scan mode 1	249±13
RTVue, scan mode 2	238±12
3D OCT-1000, scan mode 1	200±26
3D OCT-1000, scan mode 2	208±24

Sull et al, Comparison of Spectral Domain Optical Coherence Tomography Models for Assessment of Normal Macular Thickness, ARVO meeting, April 2008

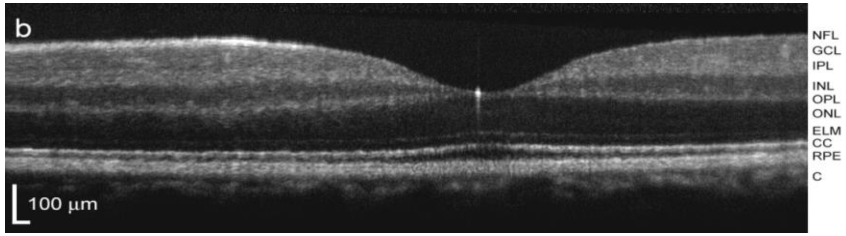

Iftimia et al, Optics Express 14(26), 2006

OCT SRM Fabrication Process

- A NIST OCT SRM consists of a triple, scattering/non-scattering/scattering, layer with controlled dimensional/optical characteristics.
- Uniform thicknesses of the layers are achieved by blade coating and spin coating of the PDMS material with known μ_a and μ_s' spectra.
- Thickness of each layer is measured by a NIST's spectral Domain (SD)-OCT with 0.9 μm axial resolution.
- For the SRM, a NIST certification for each SRM is provided with layer thickness information and their uncertainties.

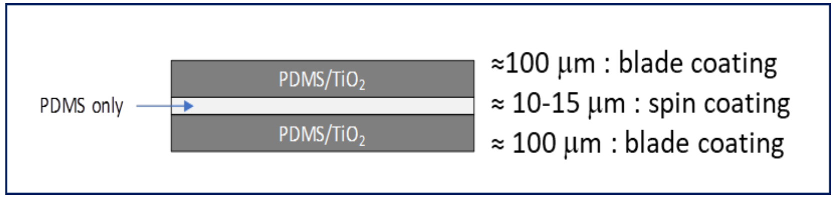

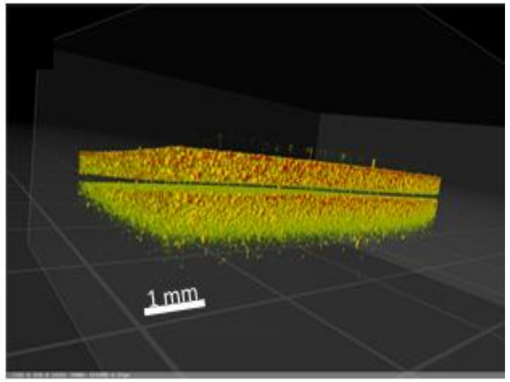

SD OCT tomography of a 3-layer phantom

Blade coating: 100 μm

Spin coating: 10-15 μm

Blade coating: 100 μm

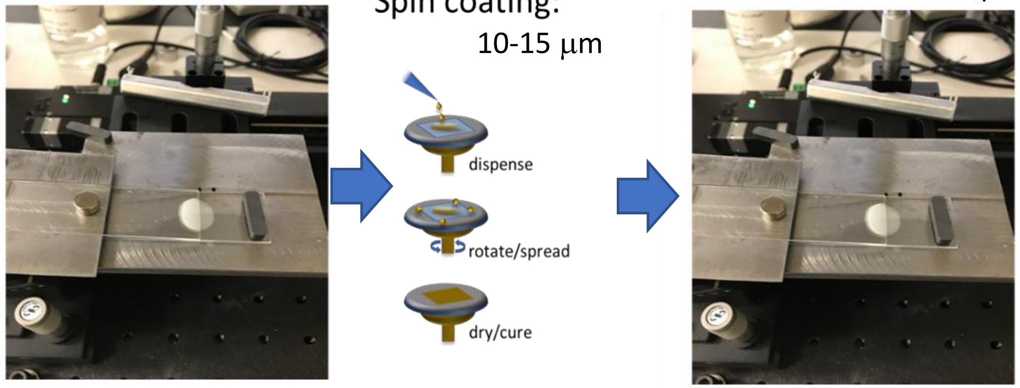

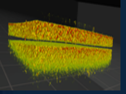

A few measurement challenges in OCT measurement standards

- In OCT, the effective path length *increases* due to the higher refractive index (RI) of the material in the path length, $l = \boldsymbol{n}c\Delta t$.
- To correct the RI factor, RI of the layered samples was measured by NIST's spectroscopic ellipsometry.
- For SI-traceability, a confocal backscatter microscopy and NIST-traceable thickness standard were used to validate the OCT results.

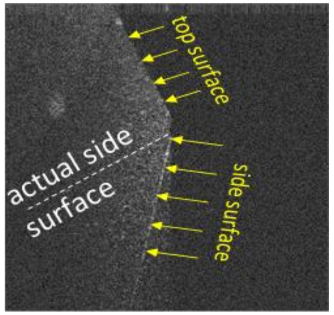

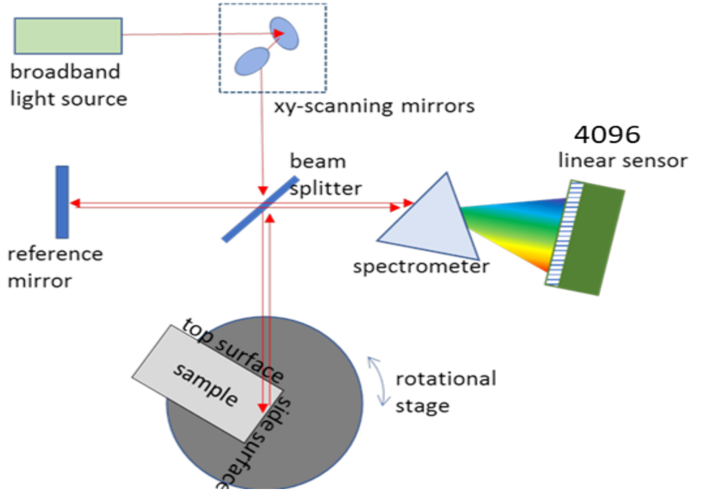

Refractive index of PDMS

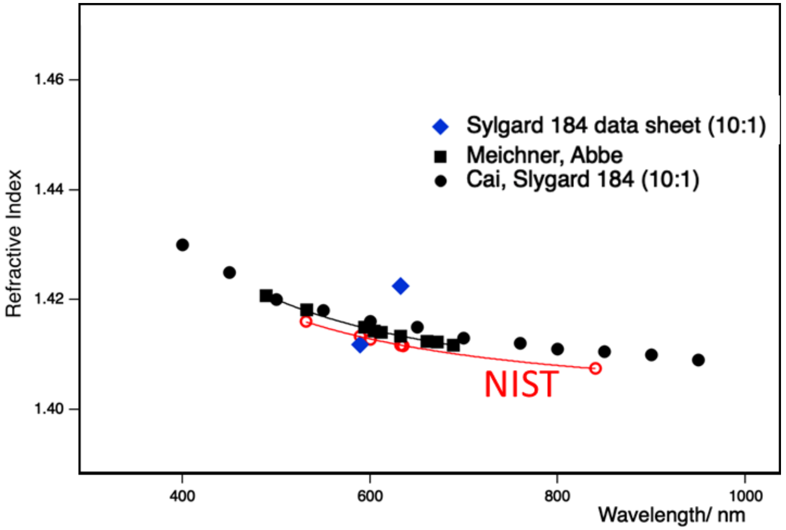

Confocal analysis of a triple layer

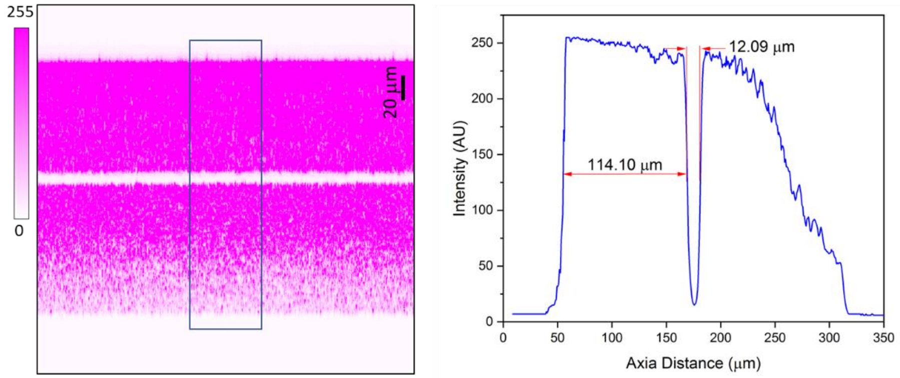

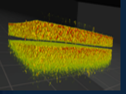

OCT aberrations (curvature) and tilt corrected

- An SRM, a 3-layer sample is on a slide with 2 mm x 2 mm grids in the back labeled to locate ROIs.
- During OCT image acquisition, sample is tilted to mitigate specular reflectance, but this tilt effect was corrected in thickness calculation algorithm for true thickness information.
- Aberrations (curvature in the image) are caused by non-linearity of scanning galvo mirrors and focusing. This artifact was also corrected.

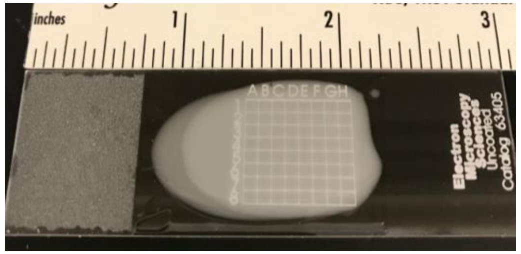

Layer tissue-simulating phantom with tunable layer thicknesses and refractive indices

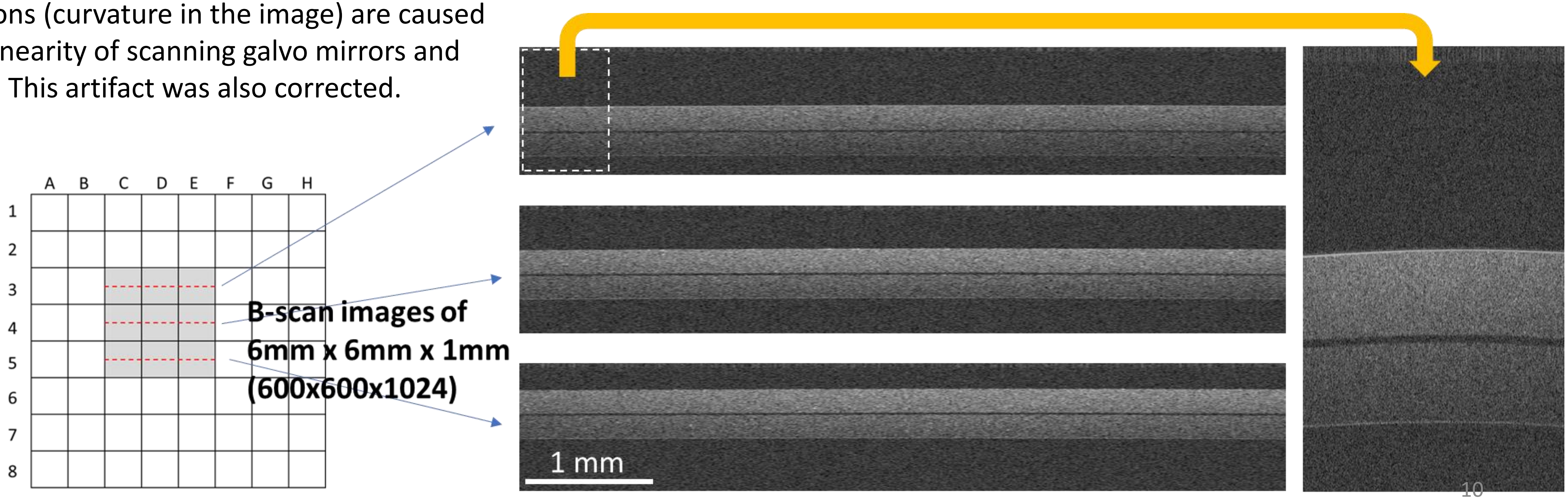

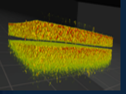

Data analysis and aberration correction algorithm

NIST

Gap Detection

Interfacial gaps are detected by a spatial operator “running” over the entire tomograph.

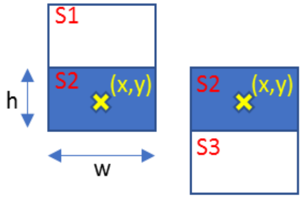

Raw tomograph

Resolved interfacial gaps

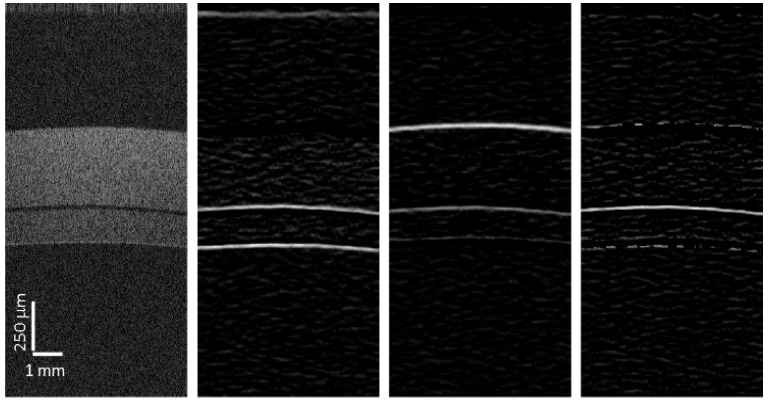

Edge Detection and Polynomial Fitting

Polynomial fitting and the quadratic equation for the curved/tilted plane is solved to find the interfacial planes in 3D.

$$z = a_0 + a_1 x + a_2 y + a_3 x^2 + a_4 y^2 + a_5 xy$$

Defined interfacial planes in 3D

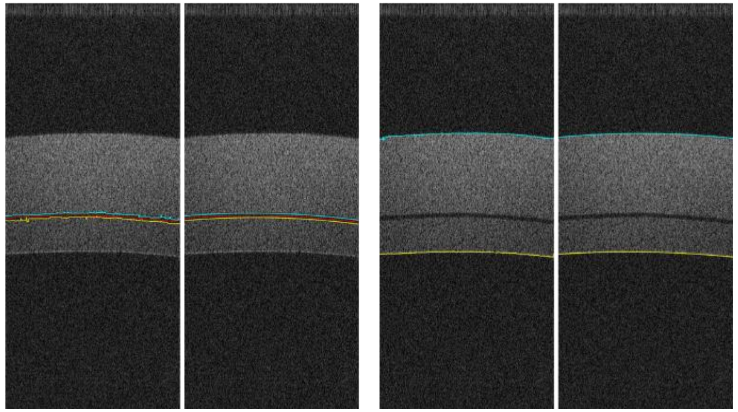

Gap thicknesses computed

The distance between the two crossing points defined by the *normal* line and upper/lower bound planes is calculated for the thickness measurements.

$$\frac{1}{n}\sqrt{l_{pp\_x}(x_1 - x_2)^2 + l_{pp\_z}(z_1 - z_2)^2}\,cos\boldsymbol{\theta}$$

Batch processing

Instrumental uncertainty of NIST’s OCT

- Theoretical axial resolution of SD-OCT: $\Delta z = \frac{1}{n_R}\frac{2\ln 2}{\pi}\frac{\lambda_{center}^2}{\Delta\lambda_{FWHM}}$ ≈ 3 μm (at 840 nm, 95 nm BW)

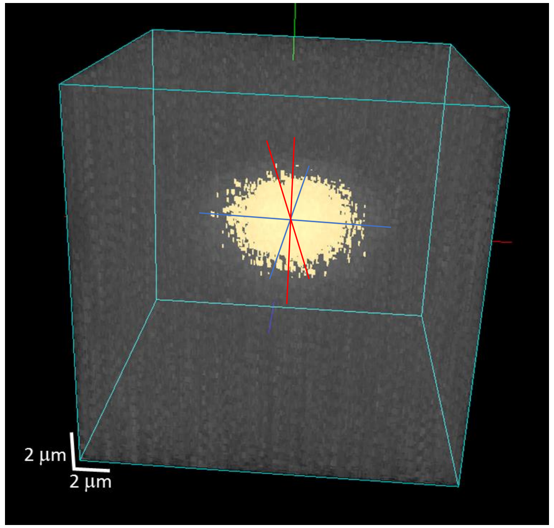

3D rendered OCT image of ***a single 40 nm*** diameter gold nanoparticle in PDMS

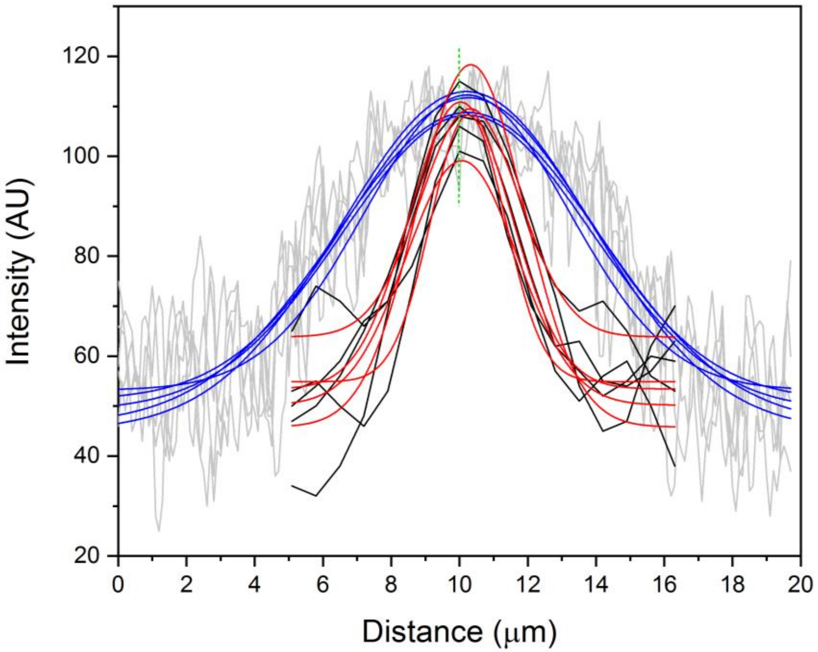

Intensity profiles crossing the center, lateral (gray) and axial (black) lines, and corresponding Gaussian fits in blue and red, respectively.

Our measurement uncertainty, based on NIST analysis algorithm, provided with the SRM is 1 μm

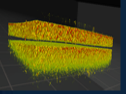

Final uncertainties for certified values

NIST

The layer thickness uncertainties are computed from the following 3 factors:

$$\frac{\delta_m}{\mu_m} = \sqrt{\left(\frac{\delta_p}{\mu_p}\right)^2 + \left(\frac{\delta_l}{l_{pp}}\right)^2 + \left(\frac{\delta_n}{n}\right)^2}$$

Uncertainty	Origin	Determination method	value
$\frac{\delta_p}{\mu_p}$	Statistical average of thickness values over a region of interest (1 mm x 1 mm area)	Standard deviation of the layer thickness by the thickness analysis algorithm	Determined for each SRM from algorithms
$\frac{\delta_l}{l_{pp}}$	Accuracy in the conversion from pixel length to the length in metric	OCT point spread function & OCT image of a metrology sample	0.015 µm / 1 µm : **1.5 %**
$\frac{\delta_n}{n}$	Measurement accuracy of the refractive index	Standard deviation of refractive index values from multiple measurements	0.001/1.408 : **0.07 %**

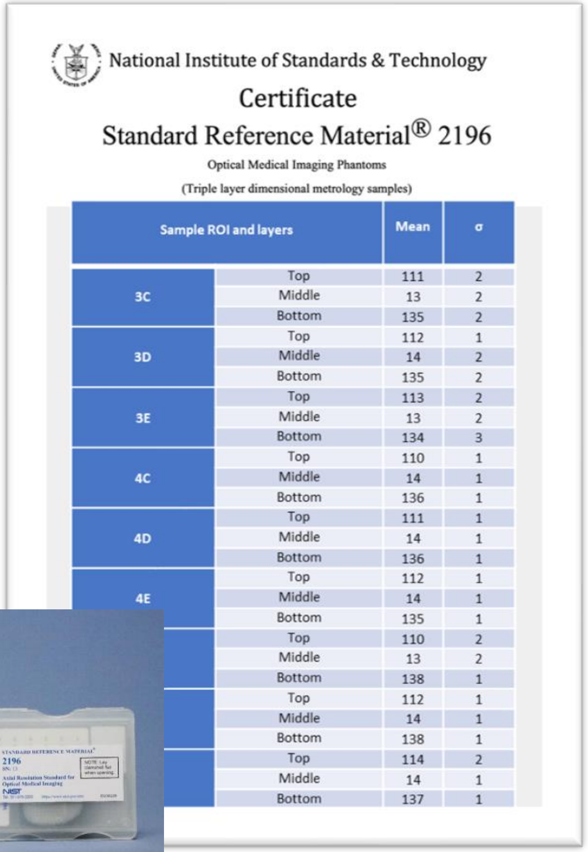

National Institute of Standards & Technology
Certificate
Standard Reference Material® 2196
Optical Medical Imaging Phantoms
(Triple layer dimensional metrology samples)

Sample ROI and layers		Mean	σ
3C	Top	111	2
	Middle	13	2
	Bottom	135	2
3D	Top	112	1
	Middle	14	2
	Bottom	135	2
3E	Top	113	2
	Middle	13	2
	Bottom	134	3
4C	Top	110	1
	Middle	14	1
	Bottom	136	1
4D	Top	111	1
	Middle	14	1
	Bottom	136	1
4E	Top	112	1
	Middle	14	1
	Bottom	135	1
	Top	110	2
	Middle	13	2
	Bottom	138	1
	Top	112	1
	Middle	14	1
	Bottom	138	1
	Top	114	2
	Middle	14	1
	Bottom	137	1

NIST SRM 2196.
https://www.nist.gov/news-events/news/2023/04/srm-verification-3d-optical-medical-imaging-devices

Type III: Standards for photoacoustic imaging (PAI)

- PAI takes advantage of low scattering of the ultrasound signal generated by pulsed photo excitation to enable label-free deep tissue imaging.
- For quantitative PAI, the measurement standards are needed for:
  - Absorption coefficient of the target
  - Local photon fluence through a scattering and absorbing medium
  - Wavelength dependent PA signal calibration
  - Transducer calibration (voltage vs P)
- NIST has developed 2D and 3D PAI phantoms for PA microscopy and PA tomography.

Absorption of Pulsed light

$$I_a = I_o\, e^{-\mu_a z}$$

Local Heating

$$\Delta T = \frac{I_a}{C_p \rho V}$$

Thermoelastic Expansion

$$V = V_o(\beta \Delta T)$$

Relaxation and Ultrasound Pressure

$$P = (\rho v_s^2)\,(\beta \Delta T)$$

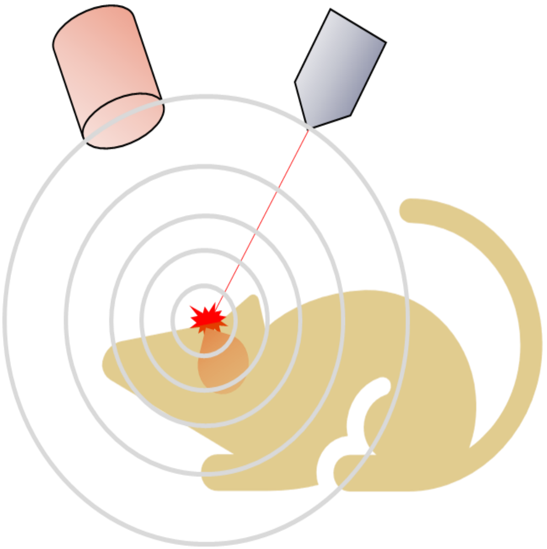

PDMS as base material for PAI phantoms

We used PDMS as base material as PDMS has:

- The largest thermoelasticity (β / C_p) as shown in the plot comparing Grüneisen parameters of different polymers
- Tunable tissue-mimicking mechanical properties
- Transparent or tunable μ'_s and μ_a with additives
- Low cost (<$10 per phantom)

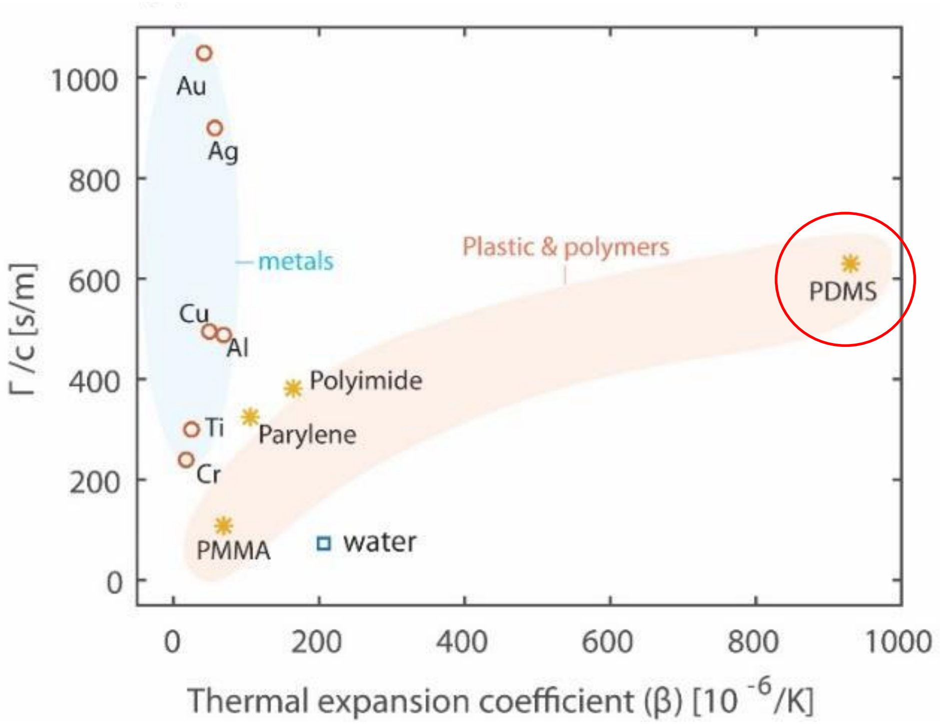

The Grüneisen parameter scaled by the speed of sound. (T. Lee, PhD. Thesis, U of Michigan Library) https://deepblue.lib.umich.edu

Vertically aligned CNT for high μ_a material

NIST

- Carbon nanotubes (CNTs) as a light absorber to imbed them into PDMS.
- CNTs are vertically grown on a silicon substrate by a CVD method and transferred to the PDMS.
- The VACNTs show a very high absorption spectra, and a flat $\mu_a(\lambda)$ over a wide wavelength range, VIS to MIR.
- Not tissue-mimicking, but these properties allow for high SNR and non-destructive PAI measurements even at high fluence.
- The PAI signal from CNTs imbedded in a PDMS with known optical properties allows for the calibration of local fluence through the medium.

CVD – grown **vertically aligned carbon nanotubes (VACNT)**

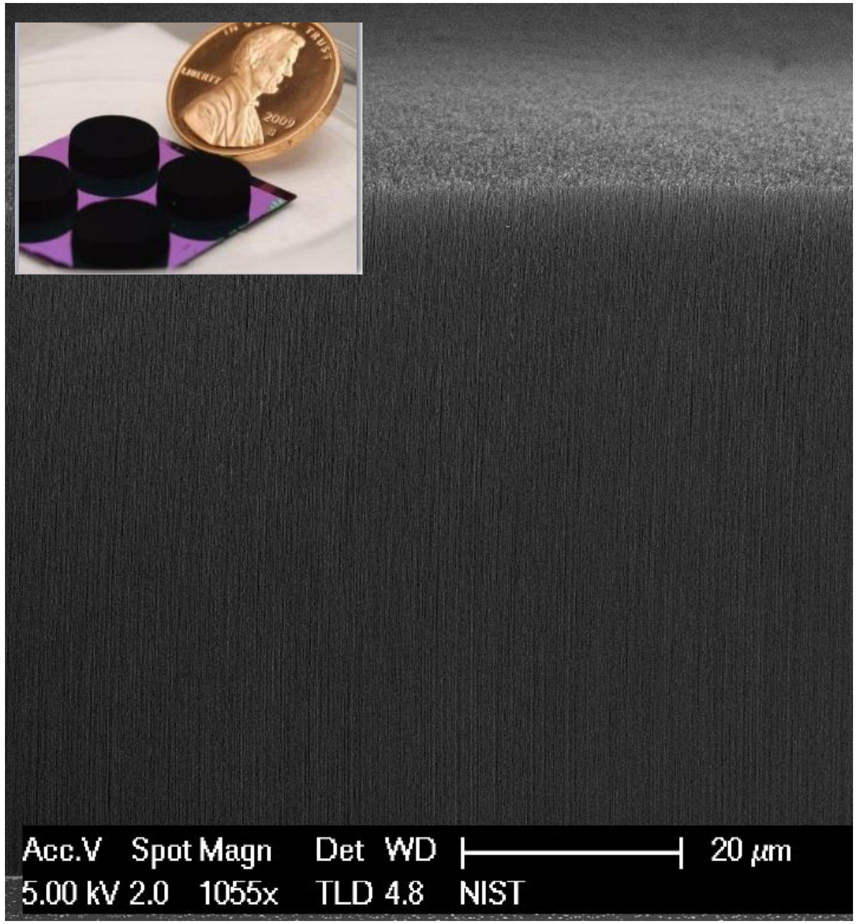

Tomlin et al, CARBON, 74 329-332 (2014)

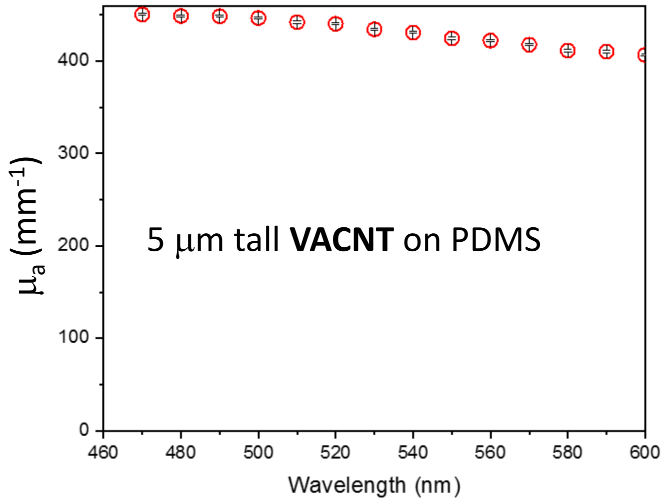

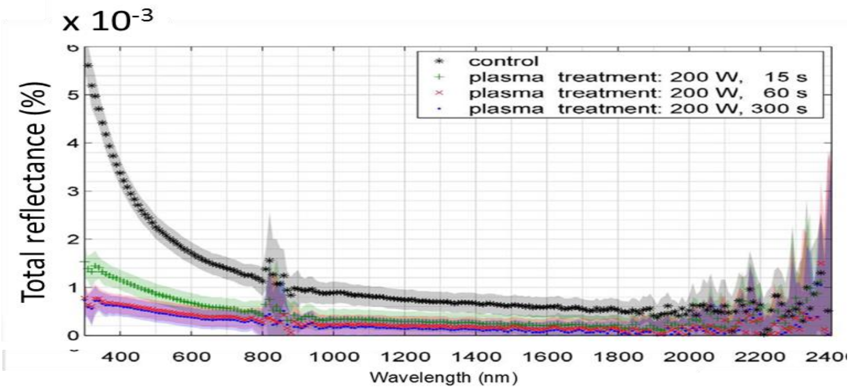

Christopher Young and John Lehman

SEM of VACNT patterns on silicon

- CVD growth of CNTs provides CNT length control so that $\mu_a(\lambda)$ can be adjusted.
- SEMs of VACNT patterns show LWR <200 nm, enabling precise patterning for resolution targets.

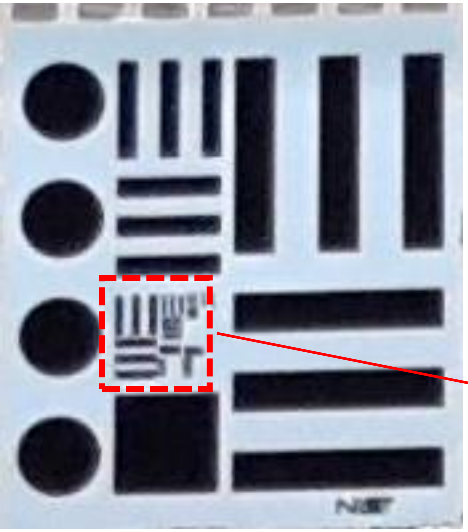

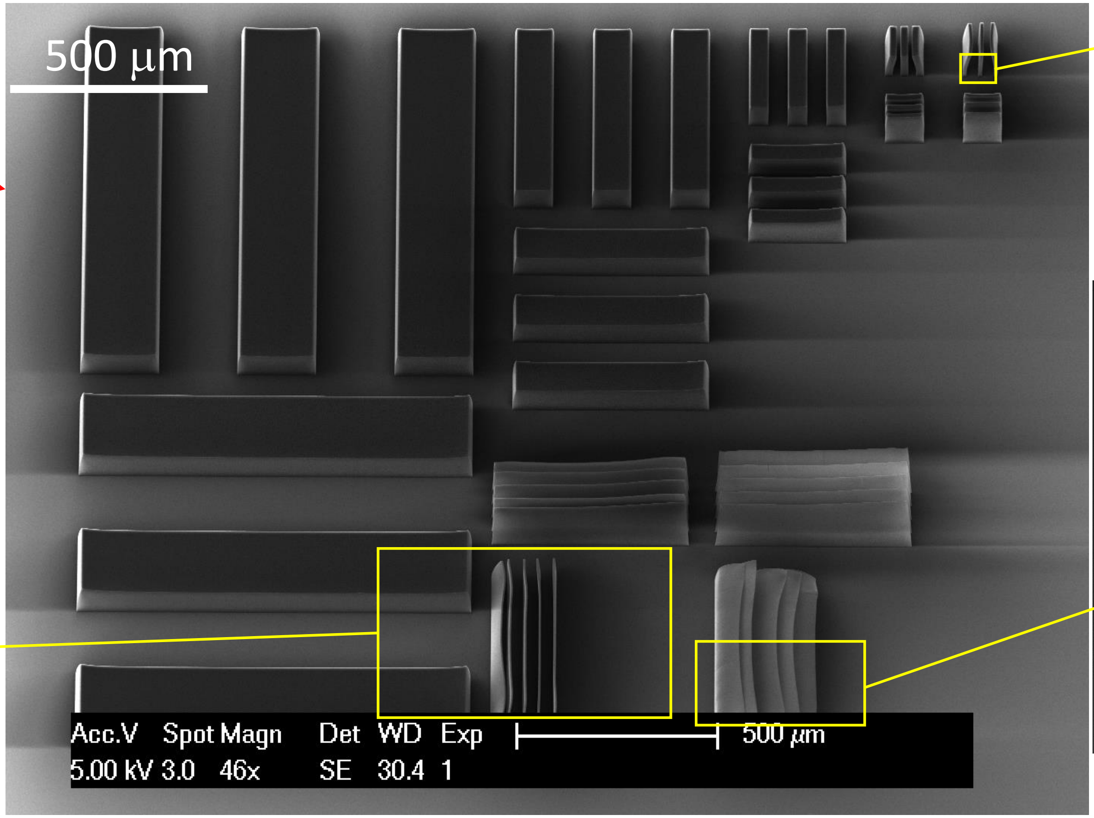

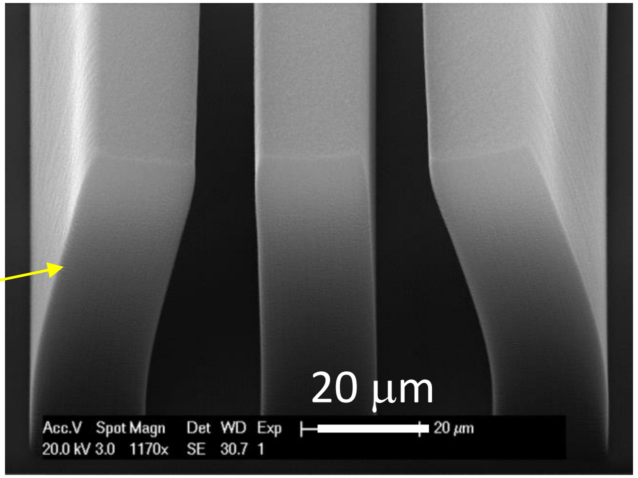

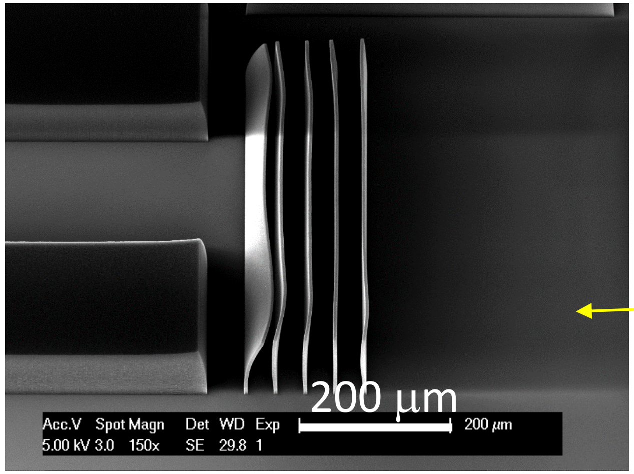

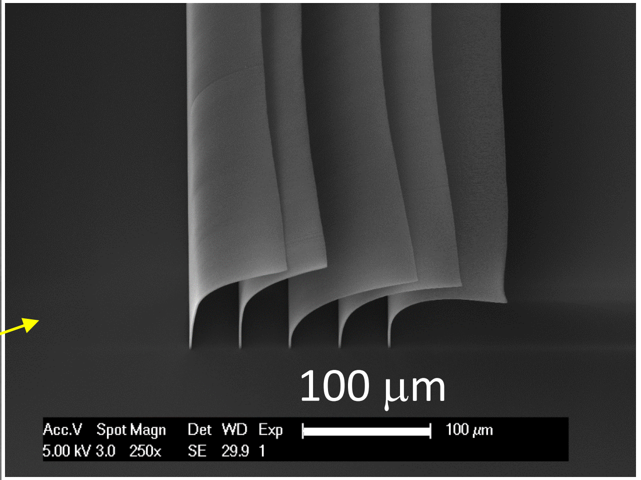

Application: Resolution target

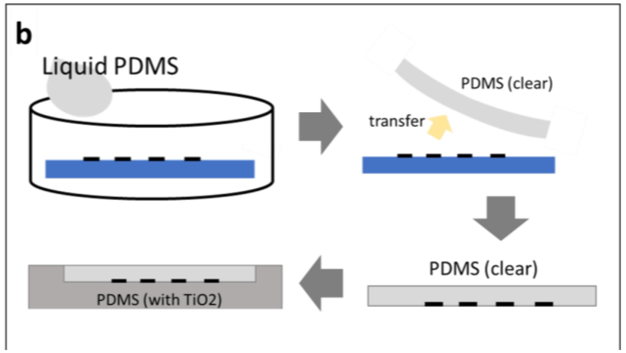

Lithographical patterns are well transferred to PDMS so the PA images from well-define patters evaluate the spatial resolution of PAI devices.

OR-PAM image of VACNTs/PDMS

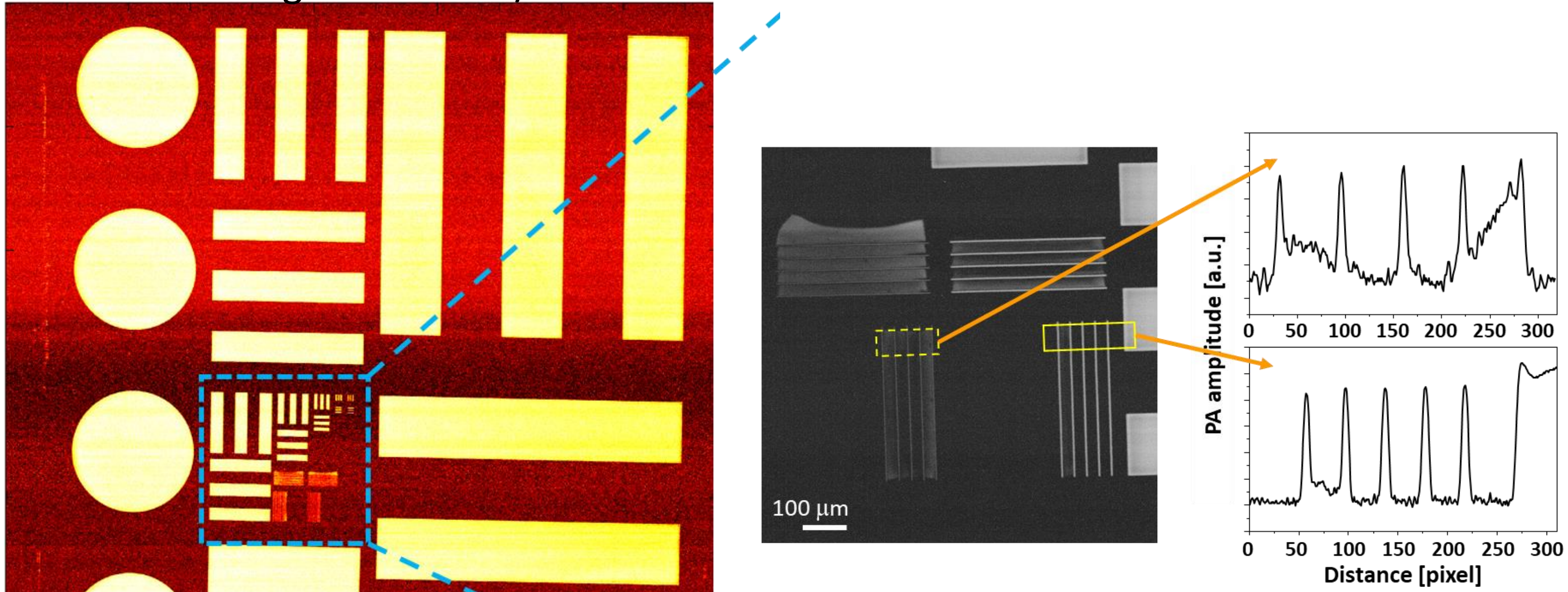

3D target for tomographic PAI

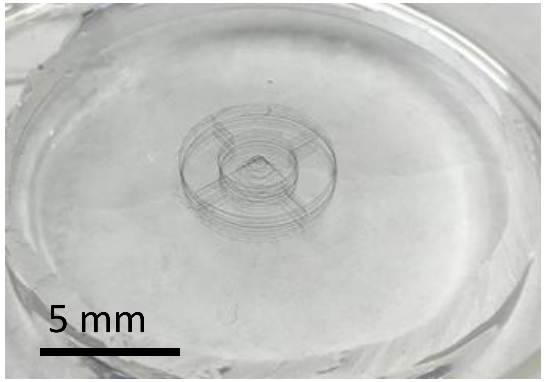

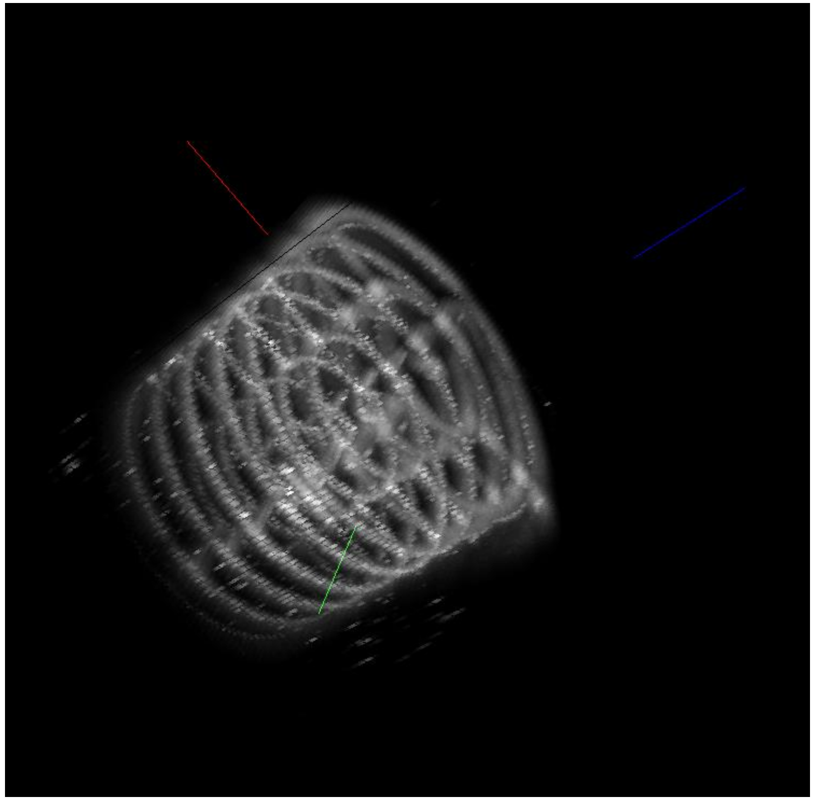

5 mm

- For 3D targets, we stack multiple 2D targets into a layer structure
- The scattering and absorption coefficients of the PDMS base material can be tuned to control the local photon fluence in 3D.
- In this picture, a 3D multilayer phantom is shown as an example: each layer contains a pattern of lines with 8 μm width, and they are designed not to block photon fluence as photons propagate through multilayers
- As we know the absorption coefficient of the patterned lines and scattering and absorption coefficient spectra of the base matrix material, local photon fluence map in 3D can be measured from the PA tomography data.
- The movie is a reconstructed tomograph from the PAI signals from the CNT patterns in multiple layers.

Summary and Acknowledgments

NIST

- ❑ NIST has developed tissue-mimicking phantoms towards standards for quantitative DOI, OCT, PAI, and hyperspectral imaging.
- ❑ Fabrication and characterization protocols are available for phantoms with characteristics presented in this paper.
- ❑ NIST has a cross-validated integrating sphere capable of measuring optical properties of tissue-mimicking phantoms
- ❑ NIST-certified SRMs for axial dimensional calibration are available for sale.

***Postdoctoral funding opportunity: visit and search for a NIST program**
https://www.nationalacademies.org/our-work/rap/nrc-research-associateship-programs

Funding

- ❑ NIST Intramural Optical Medical Imaging program
- ❑ NIST intramural Standard Development program
- ❑ NIST SBIR program
- ❑ National Research Council Associateship

Contributors

- ❑ NIST (Optical Medical Imaging Program): David Allen, Kimberly Briggman, Robert Chang, Philip Cheney, Matthew Clarke, Bonghwan Chon, Aaron Goldfain, Sangmo Kang, Hyunjin Kim, Hanh Le, Ji Youn Lee, John Lehman, Paul Lemaillet, Maritoni Litorja, Nian Liu, John Lu, Aniruddha Ray, Nikki Rentz, James Savino, Eric Shirley, Christopher Young, Helen Zhang

- ❑ External Collaborators for the NIST optical medical imaging program:

PTB Physikalisch-Technische Bundesanstalt Braunschweig und Berlin
Caltech Optical Imaging Laboratory
DARTMOUTH 1769
NATIONAL INSTITUTES OF HEALTH
THE OHIO STATE UNIVERSITY 1870
DONG-A UNIVERSITY SINCE 1946
KRISS Korea Research Institute of Standards and Science
INO
UNIVERSITY OF MICHIGAN
THE UNIVERSITY OF TEXAS AT ARLINGTON
YONSEI UNIVERSITY